

Kernel-Penalized Regression for Analysis of Microbiome Data

Timothy W. Randolph*,†, Sen Zhao#, Wade Copeland*, Meredith Hullar*, Ali Shojaie#

*Fred Hutchinson Cancer Research Center
 Biostatistics and Biomathematics
 Seattle, WA 98109

#University of Washington
 Biostatistics Department
 Seattle, WA 98195

†trandolp@fredhutch.org

March 13, 2022

Abstract

The analysis of human microbiome data is often based on dimension-reduced graphical displays and clustering derived from vectors of microbial abundances in each sample. Common to these ordination methods is the use of biologically motivated definitions of similarity. Principal coordinate analysis, in particular, is often performed using ecologically defined distances, allowing analyses to incorporate context-dependent, non-Euclidean structure. Here we describe how to take a step beyond ordination plots and incorporate this structure into high-dimensional penalized regression models. Within this framework, the estimate of a regression coefficient vector is obtained via the joint eigen properties of multiple similarity matrices, or kernels. This allows for multivariate regression models to incorporate both a matrix of microbial abundances and, for instance, a matrix of phylogenetically-informed similarities between the abundance profiles. Further, we show how this regression framework can be used to address the compositional nature of multivariate predictors comprised of relative abundances; that is, vectors whose entries sum to a constant. We illustrate this regression framework with several simulations using data from two recent studies on the gut and vaginal microbiome. We conclude with an application to our own data, where we also incorporate a significance test for the estimated coefficients that represent associations between microbial abundance and a response.

Keywords: microbial community data, penalized regression, distance-based analysis, kernel methods, compositional data.

1 Introduction

Multivariate data from genomic, metagenomic and/or metabolomic assays are often accompanied by additional information: (i) relationships between the measured *omics* features and/or

(ii) knowledge of similarities between the samples. The former may arise from network or co-occurrence structure relating the measures from p microbes, genes or metabolites [8, 16, 18] while the latter may come from a context-specific measure of dissimilarity between the n samples such as a genome-based distance [50, 66] or various measure of microbial diversity [44, 35]. The analysis of microbiome data, in particular, commonly incorporates one or both of these additional information [25, 34, 10]. Such analyses often focus on dimension-reduced graphical displays, clustering or global tests for class differences.

Comparing samples in microbiome research often begins by constructing an $n \times n$ symmetric matrix Δ of pairwise dissimilarities between the n sample profiles, each consisting of p taxon measures; see e.g., [21, 35, 55]. Principal coordinate analysis (PCoA) is then applied, plotting the n samples with respect to two or three principal components of a doubly-centered version of Δ . The choice of dissimilarity matrix and whether the data are represented as abundance of each taxon or merely presence/absence may influence the biological interpretation of the data [43, 19].

Dissimilarities that account for phylogenetic relationships among the taxa are believed to enhance statistical analyses — for instance, to improve the power of statistical tests — because they incorporate the degree of divergence between sequences [7] and do not ignore “the correlation between evolutionary and ecological similarity” [25]. The UniFrac distance [42], in particular, is based on the premise that taxa which share a large fraction of the phylogenetic tree should be viewed as more similar than those sharing a small fraction of the tree. The unweighted UniFrac distance between a pair of samples counts the number of branches in the tree that are shared by both. Evans and Matsen [15] provide an interpretation of UniFrac as one example within a larger family of Wasserstein (or earth mover’s) metrics. A closely related distance is provided by double principal coordinate analysis (DPCoA) [51] (or “generalized PCA” [54]), which also uses a phylogenetic tree to inform the covariance structure between taxa; i.e., the covariance that would arise if the data was created by the process modeled by the tree. Fukuyama et al. [19] provide an analysis and comparison of these methods. More generally, the *edge PCA* method of Matsen and Evans [46] incorporates taxon abundance information at all nodes in a phylogenetic tree (rather than just the leaves of the tree). When this is used to define a similarity between two samples (see section 3.3), the resulting kernel compares microbial samples in a manner that uses both the phylogenetic tree as well as the abundance information at the leaves, and thus may be interpreted as an extension of a PCoA with UniFrac distances.

While PCoA plots provide graphical insight into the relationship between microbial profiles and an outcome or phenotype, they do not quantify this association. More importantly, the (sets of) taxa associated with the outcome—and the magnitude or statistical significance of such associations—are not quantified by a PCoA plot. In this paper, we focus instead on estimating the association between a vector of taxon measures and an outcome using a penalized regression framework. We achieve this goal by formulating a kernel regression framework that provides a rigorous model to incorporate additional structure via similarity kernels.

We describe a general family of linear models which are constrained directly by a tree, graph or other extrinsic covariance structure, or constrained indirectly via similarity matrices. The key ingredient of this framework is the duality between distance matrices and similarity matrices discussed in section 2.1. A key emphasis of our approach is the equivalence between a taxon-based (or primal space) model and a sample-based (or dual space) formulation. This

general equivalence is well known and many of the underlying concepts presented here are simply variations of the classical theory [45]. However, a key insight we employ to connect the dual- and primal-space models is a regularization scheme due to J. Franklin [17] which allows us to formulate kernel-penalized regression models in the dual space in a manner that naturally connects to penalized estimation in the primal space; see section 2.3.

In summary, we aim to provide clarity on the models and assumptions that are tacitly implied by the many exploratory and graphically-focused PCoA analyses common in microbiome studies (section 2) and show how these models can naturally be expressed as kernel penalized regressions in either the primal (p -dimensional) variables space or the dual (n -dimensional) samples space; see sections 2.2 and 2.3. Our proposed framework leads to an approach, described in section 2.4, for addressing well-known problems that arise from applying standard (Euclidean-based) statistical models to compositional data. Section 3 illustrates the proposed framework with simulations from public data, while section 4 presents an application to our recent microbiome study of premenopausal women. In this analysis, we obtain estimates of associations between microbial species and percent fat measured in 102 premenopausal women, and also provide inference for these estimates by applying a recent significance test [70] in this kernel-penalized regression (KPR) framework.

2 From PCoA To Penalized Regression

Plots of a PCoA are commonly used in microbial ecology studies to explore relationships between samples/subjects and can be based on any dissimilarity between samples. Examples include UniFrac [42, 37, 67], DPCoA [12, 9, 47], Jenson-Shannon [13, 34] and Bray-Curtis [48, 11]. To describe our kernel regression framework, we first describe these common exploratory analyses in the general framework of “constrained ordination”.

We denote by y_i , $i = 1, \dots, n$, a quantified trait (real-valued or categorical), and by $x_i = [x_{i1}, \dots, x_{ip}]'$ a p -dimensional vector of microbial abundance values measured for each of n subjects. Denote by X the $n \times p$ sample-by-taxon matrix whose i th row is x_i . We assume throughout that the columns of X are mean centered. For now, we assume that the abundance values are appropriately normalized/transformed and postpone the treatment of compositional data to section 2.4.

2.1 PCoA and principal component regression

Consider first the Euclidean PCoA, which is simply PCA on the $n \times n$ matrix XX' . The Euclidean PCoA is thus obtained from the eigenvectors of the *kernel* matrix $K = XX'$ of inner products $K_{ij} = \langle x_i, x_j \rangle$ between samples. Now, let \mathcal{J} be the centering matrix, $\mathcal{J} = I - \frac{1}{n}\mathbf{1}\mathbf{1}'$ (where $\mathbf{1}$ is the $n \times 1$ vector of ones). Then, it can be seen that $XX' = -\frac{1}{2}\mathcal{J}\Delta\mathcal{J}$, where Δ is the $n \times n$ matrix of *squared* Euclidean distances between samples: $\Delta_{i,j} = \|x_i - x_j\|_{\mathbb{R}^p}^2$; see, e.g., [53].

The relationship between a kernel K and a distance matrix Δ is more general. In particular, if Q is a $p \times p$ symmetric, positive definite matrix used to define an inner product $\langle x_i, x_j \rangle_Q = x_i'Qx_j$ on \mathbb{R}^p , and if Δ^Q is the matrix of squared distances, $\Delta_{i,j}^Q = \|x_i - x_j\|_Q^2 = \langle x_i - x_j, x_i - x_j \rangle_Q$, defined with respect to this inner product, then $XQX' = -\frac{1}{2}\mathcal{J}\Delta^Q\mathcal{J}$ is also a similarity kernel for the n samples. We will denote this kernel by K_Q . In [54], DPCoA is identified as a generalized PCA [14], based on a distance between samples that is defined via

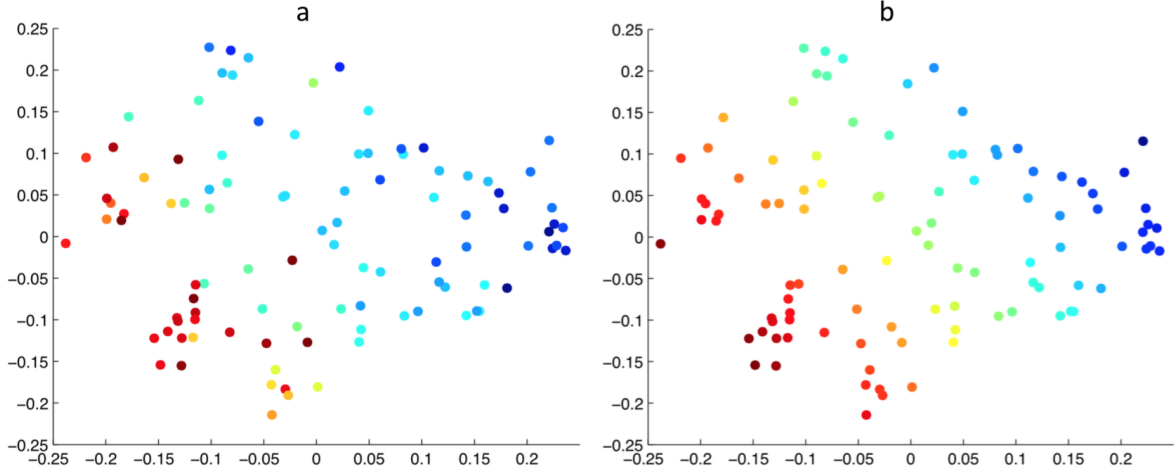


Figure 1: **PCoA plots of data from [67].** (a): PCoA plot with respect to unweighted UniFrac distance, colored according to $\log(\text{age})$ of subject. (b): PCoA plot with respect to unweighted UniFrac distance, colored according to Y_{True} from the model in Eq. (20) with $\epsilon = 0$.

the $p \times p$ matrix Q of squared patristic distances (the sum of branch lengths) between taxa. In particular, DPCoA arises simply from the principal components of $K_Q = XQX'$. Note that when Q is the identity matrix ($Q = I_p$), DPCoA reduces to the Euclidean PCoA. As emphasized in [54], the use of a non-identity Q matrix imposes structure from known relationships between the p taxa by exploiting a matrix representation of phylogenetic relationships thus providing a model for covariance structure.

In graphical explorations, two or three coordinates are typically used to explore the relationship between samples. Let $XQX' = US^2U'$ be the eigen-decomposition, with eigenvalues on the diagonal of $S^2 = \text{diag}\{\sigma_j^2\}$. Then a two-dimensional PCoA plot is the collection of points $\{\eta_{i1}, \eta_{i2}\}_{i=1}^n := \{(\sigma_1 U_{i1}, \sigma_2 U_{i2})\}_{i=1}^n$; i.e., a plot of the points represented by the first two columns of the matrix US . Often these points are colored according to a grouping label or continuous value, $\{y_i\}_{i=1}^n$, to graphically explore the existence of an association between the “response” y_i and the sample profiles summarized by the first few columns of US .

Similar graphical summaries can also be generated even if the distance does not have a quadratic form, i.e., it does not take the form XQX' . For instance, PCoA with respect to UniFrac arises from the matrix of squared UniFrac distances (either weighted or unweighted) Δ^U . Even though, in this case, Δ^U does not arise from a quadratic form, UniFrac can be seen as PCA applied to a centered version of Δ^U ; i.e., PCoA with respect to UniFrac is based on the eigenvectors of the kernel $H = -\frac{1}{2}\mathcal{J}\Delta^U\mathcal{J}$. Figure 1(a) shows an example of such a graphical display based on data from [67], where the PCoA plot is produced with respect to unweighted UniFrac distance. Here, the colors of points correspond to the logarithm of age of individual subjects.

In the case of Euclidean distance, the PCoA plot is a graphical depiction of principal component regression (PCR), where the model for the association is

$$y_i = \gamma_1 \eta_{i1} + \gamma_2 \eta_{i2} + \epsilon, \quad i = 1, \dots, n. \quad (1)$$

In Figure 1(b) the colors of individual points correspond to the “response” from eq. (1) with

$\epsilon = 0$, i.e., the response generated assuming the 2-dimensional PCR model in the unweighted UniFrac distance.

Let $A_{(k)}$ denote the first k columns of a matrix A , or k rows and columns if it is diagonal. Then, using the singular value decomposition (SVD), $X = USV'$, if we express the dimension-reduced approximation as $X \approx \tilde{X} := U_{(2)}S_{(2)}V'_{(2)}$, eq. (1) can be written as

$$\begin{aligned} y &= \gamma_1\eta_1 + \gamma_2\eta_2 + \epsilon \\ &= U_{(2)}S_{(2)}\gamma + \epsilon \\ &= \tilde{X}V_{(2)}\gamma + \epsilon, \end{aligned} \tag{2}$$

where $\gamma = [\gamma_1 \ \gamma_2]'$. Here, $\tilde{X}V_{(2)} = U_{(2)}S_{(2)}$, and $\text{Range}(\tilde{X}') = \text{Range}(V_{(2)})$. Therefore, assuming a coefficient vector β of the form $\beta = \tilde{X}'\gamma$, the model $y = \tilde{X}V_{(2)}\gamma + \epsilon$ can be written as $y = \tilde{X}\beta + \epsilon$. So inherent in a Euclidean PCoA plot is an implicit coefficient vector, β , which models a linear association between y and X . Using the SVD in (2), the PCR estimate of β is expressed as

$$\hat{\beta}_{\text{PCR}} = (\tilde{X}'\tilde{X})^\dagger \tilde{X}'y = V_{(2)}S_{(2)}^{-1}U'_{(2)}y = \sum_{k=1}^2 \frac{1}{\sigma_k} U'_k y V_k, \tag{3}$$

where \dagger denotes the Moore-Penrose inverse.

2.2 PCoA and penalized regression

An alternative to PCR is the ordinary ridge regression [29],

$$\hat{\beta}_{\text{ridge}} = (X'X + \alpha I)^{-1}X'y = \sum_{k=1}^n \left(\frac{\sigma_k^2}{\sigma_k^2 + \alpha^2} \right) \frac{1}{\sigma_k} U'_k y V_k, \tag{4}$$

in which the terms are not truncated (to, e.g., $k = 2$ in (3)) but instead re-weighted. The $\hat{\beta}_{\text{ridge}}$ estimator in (4) is the solution of the penalized least squares regression problem,

$$\hat{\beta}_{\text{ridge}} = \arg \min_{\beta} \left\{ \|y - X\beta\|_{\mathbb{R}^n}^2 + \alpha \|\beta\|_2^2 \right\}, \tag{5}$$

where α is a tuning parameter that controls the amount of shrinkage by the ridge penalty, controlling the size of β in the Euclidean (or ℓ^2) norm on \mathbb{R}^p . A number of other penalties can be used in (5). For instance, in Lasso regression [62], the least squares loss in (5) is augmented with the ℓ^1 norm of the coefficients, $\|\beta\|_1$, to encourage sparse solutions with many β_j 's being exactly zero. Multiple penalty terms can also be used, as in elastic net [71], which uses a linear combination of ℓ^1 and ℓ^2 penalties.

The above simple penalties do not account for the relationship between the p features. In particular, they would not be affected by a re-ordering of the variables' indices. Alternative penalization schemes have thus been proposed to incorporate the external information about the relationship among features. For instance, Tanaseichuk [61] uses a tree-guided penalty [33] to incorporate such structure into a penalized logistic regression framework to encourage similar coefficients among taxa according to their relationships in the phylogenetic

tree. Tibshirani and Taylor [63] study the solution path for computing a “generalized lasso” estimate in which an ℓ^2 penalty as in (5) is replaced with an ℓ^1 penalty applied to a linear transformation of the features, $\alpha\|L\beta\|_1$. Within the context of gene networks Li and Li [38] accounted for network structure by reshaping the constraint imposed by the second term of the elastic net, modifying it to be $\alpha_2\|\beta\|_{\mathcal{L}}^2 = \beta' \mathcal{L} \beta$, where \mathcal{L} denotes the graph Laplacian matrix corresponding to pre-defined connections between genes in a pathway. Here, \mathcal{L} imposes smoothness onto the estimate by penalizing the second-order difference (derivative) of β , viewing it as a function of the index parameter whose local (spatial) structure is informative. Algebraically, the structure of an \mathcal{L} -penalized estimate of β is determined by the eigen-properties of \mathcal{L} . This is discussed in [56] where a general operator, L , replaces the Laplacian \mathcal{L} and the joint eigen-structure of a pair (X, L) is the focus in studying penalties of the form $\alpha\|L\beta\|_2^2$. Heuristically, the smallest singular vectors of L and the largest singular vectors of X dominate the effect on β ; mathematically, the generalized singular vectors¹ of (X, L) span the subspace containing $\hat{\beta}$ [49, 20]. This framework thus combines the prior information on similarities, or correlations, with the empirical correlation based on the data matrix X . In what follows we consider $L'L$ and instead use a penalty of the form $Q := (L'L)^{-1}$. Specifically, we consider $\|L\beta\|^2 = \|\beta\|_{Q^{-1}} = \beta' Q^{-1} \beta$. The generalized ridge (or Tikhonov regularization [20]) estimate with respect to Q is then defined as

$$\hat{\beta}_Q = \arg \min_{\beta} \{\|y - X\beta\|_{\mathbb{R}^n}^2 + \alpha\|\beta\|_{Q^{-1}}^2\} = (X'X + \alpha Q^{-1})^{-1} X'y. \quad (6)$$

It is worth noting that, while the ridge estimate ($Q = I_p$) is biased, an informed choice of Q may, in fact, reduce bias [56]. In general, it is not necessary for Q to be invertible (or well-conditioned) since it is the dominant eigenvectors of Q that most influence the estimate. This is made clearer in the equivalent expressions below that involve Q instead of Q^{-1} .

In microbiome studies, it is often of interest to also incorporate the covariance or similarity in the space of observations \mathbb{R}^n , using a symmetric positive definite matrix H . As previously mentioned, this is the essence of PCoA, where similar to the role of Q on \mathbb{R}^p , a new inner product is considered on \mathbb{R}^n given by $\langle u, w \rangle_H = u' H w$. The corresponding norm is then defined as $\|u\|_H^2 = \langle u, u \rangle_H$. A popular example is the case of UniFrac, where $H = -\frac{1}{2} \mathcal{J} \Delta^U \mathcal{J}$ and Δ^U denotes the UniFrac distance between samples. The generalized ridge estimate $\hat{\beta}_Q$ in (6) can then be extended to incorporate structure from both H and $K = XQX'$. Formally, we consider the estimate

$$\hat{\beta}_{Q,H} = \arg \min_{\beta \in \mathbb{R}^p} \{\|y - X\beta\|_H^2 + \alpha\|\beta\|_{Q^{-1}}^2\} = (X'HX + \alpha Q^{-1})^{-1} X'Hy, \quad (7)$$

where the estimate is informed by both Q and H .

To relate this estimator with existing approaches, and develop its kernel regression counterpart, it will be useful to express (7) as:

$$\begin{aligned} \hat{\beta}_{Q,H} &= Q(X'HXQ + \alpha I_p)^{-1} X'Hy \\ &= QX'(XQX' + \alpha H^{-1})^{-1} y, \end{aligned} \quad (8)$$

¹We refer here to the generalized singular value decomposition (GSVD) of Van Loan [40] which is a simultaneous decomposition of two matrices. A different generalization of the SVD [22] imposes constraints on left and right singular vectors of a matrix.

where here and throughout the following basic identities are useful:

$$\begin{aligned} (X'HX + Q^{-1})^{-1}X'H &= (QX'HX + \alpha I_p)^{-1}QX'H = Q(X'HXQ + \alpha I_p)^{-1}X'H \\ &= QX'(XQX' + H^{-1})^{-1} = QX'H(XQX'H + \alpha I_n)^{-1}. \end{aligned} \quad (9)$$

Special cases of (7) are worth considering. For instance, $H = I_n$ corresponds to generalized ridge regression using a penalty defined by Q as in (6). Moreover, in view of the identities in (9), $\hat{\beta}_{Q,H}$ can be seen as kernel ridge regression with respect to the DPCoA matrix $K_Q = XQX'$ [54]: $\hat{\beta}_{Q,H} = QX'\hat{\gamma}$, where $\hat{\gamma} = (K_Q + \alpha I_n)^{-1}y$. This is discussed further in the next section along with the case of $H \neq I_n$, which corresponds to the essence behind weighted or generalized least squares regression. In particular, the classical generalized least square (GLS) estimate can be recovered from an unpenalized regression by setting $H = \Sigma^{-1}$, where $\Sigma = \mathbb{E}(\epsilon\epsilon')$ is the covariance matrix of the noise. A ridge-like constraint then leads to the GLS-ridge estimate $\hat{\beta}_{\text{GLS ridge}} = \arg \min_{\beta \in \mathbb{R}^p} \{ \|y - X\beta\|_{\Sigma^{-1}}^2 + \alpha \|\beta\|^2 \}$, also discussed in [45].

2.3 Kernel-penalized regression

In the high-dimensional setting, where $p \gg n$, the estimation of $\hat{\beta}_{Q,H}$ in (7) in the data space \mathbb{R}^p can be computationally inefficient. In the case of a standard ridge penalty, kernel ridge regression estimation facilitates estimation and prediction by solving an equivalent optimization in the dual space \mathbb{R}^n [57]. In this section, we show that $\hat{\beta}_{Q,H}$ can be similarly obtained by exploiting the “kernel trick” and solving an optimization problem in \mathbb{R}^n .

Consider first the case of ordinary ridge regression, where $H = I_n$ and $Q = I_p$. In this case, an estimate of β can be obtained as $\hat{\beta}_{\text{ridge}} = X'\hat{\gamma}_{\text{kernel ridge}}$, where

$$\hat{\gamma}_{\text{kernel ridge}} = (K + \alpha I)^{-1}y = (K^2 + \alpha K)^{-1}Ky = \arg \min_{\gamma \in \mathbb{R}^n} \{ \|y - K\gamma\|^2 + \alpha \|\gamma\|_K^2 \}. \quad (10)$$

One way to generalize the estimate in (10) to include $H \neq I_n$ is to define the penalty in terms of H as

$$\hat{\gamma}_* = (K^2 + \alpha H^{-1})^{-1}Ky = \arg \min_{\gamma} \{ \|y - K\gamma\|^2 + \alpha \|\gamma\|_{H^{-1}}^2 \}, \quad (11)$$

which is exactly the commonly-used Tikhonov regularization in the dual space (compare eq. (6)). Unfortunately, $\hat{\gamma}_*$ has no obvious connection to a penalized estimate of β and cannot be used to derive an estimate of β in the primal space.

To bridge this gap, we consider instead an *alternative regularization principle* introduced by Franklin [17] in the context of differential equations. Let $\hat{\gamma} := (XQX' + \alpha H^{-1})^{-1}y$. It is then easy to see that $\hat{\beta}_{Q,H} = QX'\hat{\gamma}$. Then $\hat{\gamma}$ is the coefficient estimate from a kernel penalized regression problem. Specifically, for $K = XQX'$, it can be shown that

$$\hat{\gamma} = (K + \alpha H^{-1})^{-1}y = \arg \min_{\gamma \in \mathbb{R}^n} \{ \|y - K\gamma\|_{K^{-1}}^2 + \alpha \|\gamma\|_{H^{-1}}^2 \}, \quad (12)$$

or equivalently,

$$\hat{\gamma} = (HK + \alpha I_n)^{-1}Hy = \arg \min_{\gamma \in \mathbb{R}^n} \{ \|y - K\gamma\|_H^2 + \alpha \|\gamma\|_K^2 \}. \quad (13)$$

Comparing (13) and (11), one sees that the analytic form of the Franklin regularization involves just K , rather than $K'K = K^2$ in its Tikhonov counterpart. When $H = I$, the

regularization in (13) reduces to the kernel-ridge estimate in (10), but even when $H \neq I$, we can recover a primal-space estimate of β . Thus, the proposed regularization framework is a natural choice in the setting of kernel-penalized regression.

We further clarify the roles being played by the two kernels K and H . In general, a sufficient condition for a matrix, K , to be a similarity kernel is that it is induced by a feature map $\phi: \mathbb{R}^p \rightarrow \mathcal{K}$, the i, j entry of K defined as the inner product of the observations $x_i \in \mathbb{R}^p$, but calculated with respect to their transformed versions $K_{ij} = \langle \phi(x_i), \phi(x_j) \rangle$ in the new inner product space, \mathcal{K} . Examples include $K = XX'$ or $K = XQX'$, where \mathcal{K} is \mathbb{R}^p with inner product $\langle \cdot, \cdot \rangle_Q$ (as in DPCoA) and it is this quadratic form that we require for K , above. H , on the other hand, may be any symmetric positive semi-definite matrix. For our purposes, we are more interested in biologically-motivated kernels (e.g., those derived from the phylogenetic tree as in Sections 3.2 and 3.3) than mathematically-derived ones (e.g., polynomial or Gaussian). The proposed regularization scheme of (12) allows us to relate the coefficient estimates of primal and dual spaces, $\hat{\beta}_{Q,H} = QX'\hat{\gamma}$, even when $H \neq I$.

It is also useful to observe that the roles of K and H in the estimate $\hat{\gamma}$ can be expressed explicitly in terms of the generalized eigenvalues and eigenvectors of the pair (K, H^{-1}) . Specifically, let w_1, \dots, w_n denote the columns of the matrix W for which $W'KW = \text{diag}\{\sigma_1, \dots, \sigma_n\}$ and $W'H^{-1}W = \text{diag}\{\mu_1, \dots, \mu_n\}$. That is, if $\{w_k\}$ denotes a basis with respect to which a simultaneous diagonalization of K and H^{-1} is obtained (see [20, 27]), then

$$\hat{\gamma} = \sum_{k=1}^n \left(\frac{\sigma_k}{\sigma_k + \alpha\mu_k} \right) \frac{w_k'y}{\sigma_k} w_k. \quad (14)$$

This alternative expression is a consequence of the Franklin regularization in (12) and explicitly reveals the role of H in the penalized regression models. Since H is invertible, the w_k 's are also eigenvectors of HK [20]. I.e., the estimates in (12) and (7) arise from the matrix product of two kernels.

Another observation is that the penalty term in (12) serves not necessarily to regularize an *ill-posed* problem, but to incorporate information from both K and H into the regression model. In this view, K and H are presumed to exhibit a shared eigen-analysis; both may be informative, for example, with respect to classifying samples, as discussed in section 3.3 (see Figure 4). Indeed, it is popular to consider a more than one definition of (dis)similarity in the analysis of microbiome data with the presumption that they provide different, but compatible, views of the data. Here we have loosely referred to H and K as being “co-informative”, but this can be quantified by the Hilbert-Schmidt information criteria (HSIC) [24, 23] or its relatives such as the RV statistic [32] or the distance covariance [60]; see the survey [31]. The HSIC for the dependence of two data sets, X and Z , is based on the eigen-spectrum of covariance operators defined by two kernels, K and H , respectively. The empirical HSIC is simply $\text{trace}(HK)$.

2.4 Regression with Compositional Data

When counts are obtained from genomic surveys such as 16S rRNA gene profiling, normalizing the raw count data is necessary because the total number of reads per sample can vary by several orders of magnitude. Common approaches for normalizing these data include converting them to proportions (relative percent) or subsampling the sequences to create

equal library sizes for each sample (rarifying). These data are “compositional” in the sense that the microbial abundances represent a proportion of a constant total. It is well known, however, that this can result in spurious correlations among taxa [1, 18] and when there are a few dominant taxa, the problem of artificial correlations can be quite extreme.

Compositional data reside on the *simplex* S^{p-1} of unit-sum vectors in \mathbb{R}^p and so standard multivariate methods do not apply [2, 52, 39, 41]. In particular, because these data do not naturally reside in a Euclidean vector space, standard regression models based on Euclidean covariance measures are inappropriate. This is highlighted by ordinary least-squares and ridge regression in which coefficient estimates, being of the form $\hat{\beta} = (X'X + \alpha I)^{-1}X'y$, depend on the empirical covariance structure, $X'X$, between taxa. Similarly, Li [39] points out that a naive application of lasso regression is not expected to perform well due to the compositional nature of the covariates. He addressed this by applying a lasso regression model to the log-ratio abundances and imposing an additional constant-sum constraint on the coefficient vector, β . Here we propose an approach that uses the centered log-ratio transformation of the compositional vectors and an estimate of covariance among the log taxa counts that is obtained via Aitchison’s variance matrix [2, 52].

Let X be the $n \times p$ sample-by-taxon matrix whose rows are relative percent (compositional) vectors $\{x_i\}_{i=1}^n$; its columns will be denoted by x^k , corresponding to $k = 1, \dots, p$ taxa. Let $g(x) = (\prod_{k=1}^p x^k)^{1/p}$ be the geometric mean of a row vector, x , and denote the centered log-ratio (CLR) transform of x_i by $\tilde{x}_i = \text{clr}(x_i) := \left[\log \frac{x_i^1}{g(x_i)}, \dots, \log \frac{x_i^p}{g(x_i)} \right]$. In what follows we use the matrix of CLR vectors, \tilde{X} , and the normalized variation matrix T , of X , as defined by Aitchison [3]: $T_{k,\ell} = \text{var} \left(\frac{1}{\sqrt{2}} \log \frac{x^k}{x^\ell} \right)$. T is a symmetric dissimilarity matrix with zeros on the diagonal and entries that have squared Aitchison distance units: the Aitchison norm of a vector x in the simplex S^{p-1} is defined as $\|x\|_a^2 = \frac{1}{2p} \sum_{k,\ell} \left(\log \frac{x^k}{x^\ell} \right)^2$. In fact, $\|x\|_a^2 = \|\text{clr}(x)\|^2$. One can show that T is related to the covariance matrix, C of the log of the true taxa counts (which are not observed) as $T = v\mathbf{1}' + \mathbf{1}v' - 2C$ [39]. Consequently, $C = -\frac{1}{2}\mathcal{J}T\mathcal{J}$, and we can use C in place of Q in eq. (6):

$$\hat{\beta} = \arg \min_{\beta} \{ \|y - \tilde{X}\beta\|_{\mathbb{R}^n}^2 + \alpha \|\beta\|_{C^{-1}}^2 \}. \quad (15)$$

As a comparison, we observe that Li [39] proposed a constrained regression

$$E(y_i) = \beta_1 \log x_i^1 + \dots + \beta_p \log x_i^p \quad \text{subject to } \sum_{j=1}^p \beta_j = 0, \quad (16)$$

with a lasso penalty to obtain an estimate of the form

$$\arg \min_{\beta} \left(\frac{1}{2n} \|y - \sum_j \log(x^j)\beta_j\|_{\mathbb{R}^n}^2 + \lambda \sum_j |\beta_j| \right) \quad \text{subject to } \sum_{j=1}^p \beta_j = 0.$$

The zero-sum constraint on β was emphasized for interpretability advantages over the standard lasso estimate. Temporarily denoting $\beta_p = -\sum_{j=1}^{p-1} \beta_j$, we see that (16) is equivalent

to

$$\begin{aligned} \mathbb{E}(y_i) &= \beta_1 \log \frac{x_i^1}{x_i^p} + \beta_2 \log \frac{x_i^2}{x_i^p} + \cdots + \beta_{p-1} \log \frac{x_i^{p-1}}{x_i^p} \\ &= \beta_1 \log x_i^1 + \beta_2 \log x_i^2 + \cdots + \beta_{p-1} \log x_i^{p-1} - \sum_{j=1}^{p-1} \beta_j \cdot \log x_i^p. \end{aligned}$$

Since $\sum_{j=1}^p \beta_j = 0$, this can be rewritten as

$$\begin{aligned} \mathbb{E}(y_i) &= \beta_1 \log x_i^1 + \cdots + \beta_p \log x_i^p - \left(\sum_{j=1}^p \beta_j \right) \log g(x_i) \\ &= \beta_1 \log \frac{x_i^1}{g(x_i)} + \cdots + \beta_p \log \frac{x_i^p}{g(x_i)} \quad \text{subject to } \sum_{j=1}^p \beta_j = 0. \end{aligned}$$

Therefore, Li's proposal of regression on log-ratio abundances is equivalent to regression on the CLR-transformed data \tilde{X} provided a zero-sum constraint is imposed on β . In contrast, however, our formulation does not explicitly impose a constant-sum constraint. This is not needed because the CLR transform removes the analysis from the simplex to allow an analysis in Euclidean vector space algebra [52]. Our model then incorporates the appropriate covariance structure via C .

Finally, we note that a positive-definite C in (15), or more generally Q in (6), can be decomposed as a sum $Q = I + \tilde{Q}$ of the identity plus a positive semi-definite singular matrix \tilde{Q} . The identity term constrains $\sum_{j=1}^p \beta_j^2$ to be small while, overall, \tilde{Q} encourages extrinsic structure (e.g., smoothness). One may also control the size of $\sum_{j=1}^p \beta_j^2$ by adding or subtracting values in the diagonal entries of Q . This idea is similar to that of "Grace-ridge" in Zhao and Shojaie [70] where, in addition to the penalty induced by Q , the authors propose to further impose a ridge-type penalty in the objective. We apply the significance testing framework of [70] in section 4.

3 Numerical Experiments

To illustrate the proposed framework, we perform several data-driven simulations using published microbiome data. We consider three scenarios from the literature that exploit extrinsic structure from a phylogenetic tree, including DPCoA, UniFrac and edge PCA. To achieve realistic simulations, we simulate "true" signal of the type implied by each of these methods in order to create benchmarks for evaluating performance. Our emphasis is on formalizing the role that such structure plays in penalized regression when modeling associations between the multivariate data, X , and a response variable, y . Since y is directly simulated from X in these settings, the compositional nature of the data discussed in section 2.4 does not affect the simulation results. We will return to this topic when analyzing the relative abundance data in section 4.

The numerical experiments in this section are motivated by the relationship between the PCoA plots and PCR described in section 2.1 and Figure 1. This connection can be generalized to a number of other commonly-used graphical representations in the microbiome literature.

For instance, in any two-dimensional DPCoA plot there is an implicit coefficient vector, β , of associations between y and X . If Q is positive definite with a Cholesky decomposition $Q = LL'$, this estimate $\hat{\beta}_{\text{PCR},Q}$ takes the same form as $\hat{\beta}_{\text{PCR}}$ in Eq. (3), but now the vectors U_k and V_k arise from the SVD of $XL = USV'$. Here, $XQX' = (XL)(XL)'$ so U and S are the same matrices as in the eigen-decomposition $K_Q = XQX' = US^2U'$, above. Hence, a regression estimate for β that is implicit in the DPCoA plot can be obtained via kernel ridge regression:

$$\hat{\gamma}_Q = (K_Q + \alpha I)^{-1} = \arg \min_{\gamma \in \mathbb{R}^n} \{ \|y - K_Q \gamma\|^2 + \alpha \|\gamma\|_{K_Q}^2 \} \quad (17)$$

and then denoting $X_L = XL$,

$$\hat{\beta}_{\text{DPCoA}} = X_L' \hat{\gamma}_Q = L' X' (XQX' + \alpha I)^{-1} y = L' (X' X + \alpha Q^{-1})^{-1} X' y = L' \hat{\beta}_Q, \quad (18)$$

where $\hat{\beta}_Q$ is defined explicitly in (6). Further, in analogy to (4), a non-truncated basis expansion of $\hat{\beta}_Q$ can be written as:

$$\hat{\beta}_Q = \sum_{k=1}^n \left(\frac{\sigma_k^2}{\sigma_k^2 + \alpha \mu_k^2} \right) \frac{1}{\sigma_k} U_k' y V_k, \quad (19)$$

where here σ_k , μ_k , and U_k , V_k are the *generalized* singular values and vectors [49, 20] of the pair (X, L^{-1}) [56].

Throughout this section, we compare the performance of KPR methods with ridge regression, which provides the most similar and interpretable extension of an ordinary least squares estimate. Ridge regression thus provides a natural benchmark for comparing various KPR estimates. On other hand, given that in our simulations the signal is simulated to reflect the extrinsic structure of the data, it is unfair to compare a method that does not use such structure with one that does. In particular, a sparsely estimated $\hat{\beta}$ from lasso does a poor job capturing localized structure in a β inherent in DPCoA, for example, and is hence not considered. Our choice of competing methods is also limited by the emphasis of the paper on estimation of β , rather than prediction of the outcome y , which, e.g., renders many available kernel regression methods inappropriate.

In all simulation experiments, the tuning parameters for KPR and ridge regression are chosen using 10-fold cross-validation. Specifically, to compare the prediction performance between KPR and ridge regression, we choose the tuning parameters that minimize squared test error in held out cross validations. On the other hand, the task of estimation usually requires more smoothing than prediction [6]. Therefore, when considering the estimation performances of both KPR and ridge regression, we use the largest tuning parameters such that the squared test errors are within one standard error of the minimum squared test error, as suggested in [28]. For comparison, we also considered the tuning parameters corresponding to the minimum squared test error for ridge regression.

3.1 Regression and DPCoA

In our first example, we compare the estimation and prediction performance of KPR and ridge regression using the data depicted in Figure 1. The data contain relative abundances for $p = 149$ taxa from $n = 100$ subjects in a study by Yatsunenko et al. [67]. The outcome y is the log-transformed age for each subject. For KPR, we use $K_Q = XQX'$ and $H = I$, where Q is

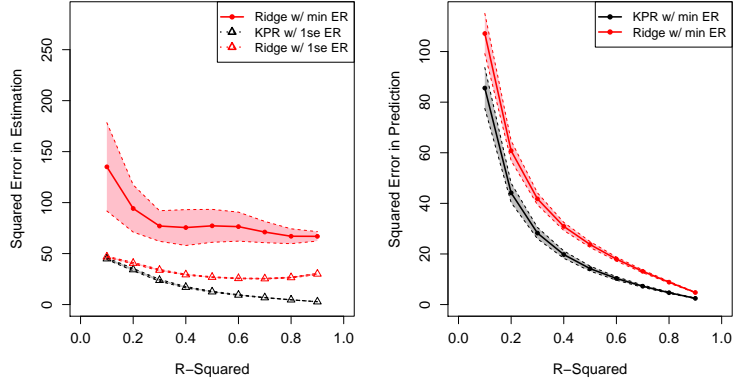


Figure 2: DPCoA average estimation and prediction squared errors of KPR (black) and ridge regression (red), and their 95% confidence bands. Tuning parameters are the ones that produce the smallest squared test error (min ER), and the largest ones such that the squared test errors are within one standard error of the minimum squared test error (1se ER).

the Brownian motion matrix obtained from the patristic distances between the tips of the tree for each pair of taxa. Motivated by DPCoA plots, we assume the underlying “true” response y_{True} comes from the first two eigenvectors of K_Q . A PCoA plot with this idealized response is shown in Figure 1(b). We estimate $\hat{\beta}_{\text{DPCoA}}$ according to (18), and estimate $\hat{\beta}_{\text{Ridge}}$ using the same equation with $Q = I$. We get $\tilde{y}_{\text{DPCoA}} = XL\hat{\beta}_{\text{DPCoA}}$ and $\hat{y}_{\text{Ridge}} = XI\hat{\beta}_{\text{Ridge}}$, where L comes from the Cholesky decomposition of Q , $Q = LL'$. We repeat the process 400 times, each with a different $\epsilon \sim N_n(0, \sigma_\epsilon^2 I_n)$ in (2). σ_ϵ^2 is derived to achieve $R^2 = \text{var}(y_{\text{True}})/(\text{var}(y_{\text{True}}) + \sigma_\epsilon^2) \in \{0.1, 0.2, \dots, 0.9\}$. The performance metrics are the squared difference of the estimates from y_{True} for prediction and from β_{True} for estimation, where β_{True} denotes the regression coefficients in the space of XL , i.e. $y_{\text{True}} = XL\beta_{\text{True}}$.

Figure 2 shows the estimation and prediction performance of KPR and ridge regression. KPR significantly outperforms ridge regression for both prediction and estimation in all settings. Note that, as expected, ridge regression also performs better when using a larger tuning parameter (minimum squared test error plus one standard error) than simply using the smallest squared test error.

3.2 Regression and PCoA with respect to a UniFrac kernel

In the case of PCoA with respect to a UniFrac or other matrix Δ of squared dissimilarities, the graphical displays are based on the eigen-decomposition of $H = -\frac{1}{2}\mathcal{J}\Delta\mathcal{J}$. That is, for $H = US^2U' \approx U_{(2)}S_{(2)}^2U'_{(2)}$, the n samples are represented in two-dimensions by the columns of $U_{(2)}S_{(2)}$; one plots the collection of points $\{\eta_{i1}, \eta_{i2}\}_{i=1}^n := \{(\sigma_1 U_{i1}, \sigma_2 U_{i2})\}_{i=1}^n$, as in Figure 1. When the points are colored according to a response variable, $\{y_i\}_{i=1}^n$, the implied regression model is

$$\begin{aligned} y &= \gamma_1 \eta_{i1} + \gamma_2 \eta_{i2} + \epsilon \\ &= U_{(2)}S_{(2)} \gamma + \epsilon. \end{aligned} \tag{20}$$

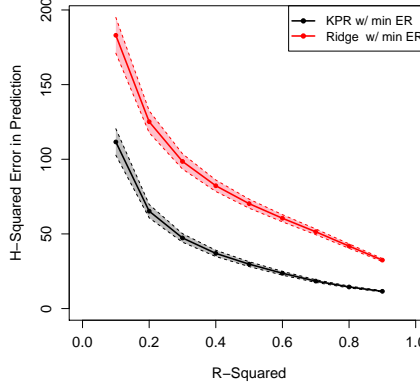


Figure 3: UniFrac average prediction H -squared error of KPR (black) and ridge regression (red), with the 95% confidence bands. Tuning parameters are the ones that produce the smallest test error (min ER).

However, in contrast to (2) where we used $US = XV$, we cannot connect γ directly to the p -coordinates in the columns of X . Said another way, one *could* proceed as in (17) by simply replacing K_Q by H , but the resulting estimate $\hat{\gamma}$ would have no clear connection with a principled estimate of β . Instead of replacing K_Q , one can exploit the joint eigenanalysis of the kernels K_Q and H (see (14)) by proceeding as in (13), leading to the estimate $\hat{\beta}_{Q,H} = X'\hat{\gamma}$ in (8) which is a GLS-type extension of generalized ridge regression.

In this example, we use the same data as in section 3.1. For KPR, we use $K = XX'$ and H is obtained from the UniFrac distance metric. We calculate the “true” γ_{True} and y_{True} from (20) and the estimated $\hat{\gamma}$ from (12). This bivariate regression is illustrated in Figure 1(b) and serves as a “true” (known) relationship that we aim to estimate. Similar to the last example, we repeat the process 400 times, each with a different $\epsilon \sim N_n(0, \sigma_\epsilon^2 I_n)$ in (20) to simulate various values of $R^2 \in \{0.1, 0.2, \dots, 0.9\}$. The performance metric is the H -squared error, which is defined as $\|\hat{y} - y_{\text{True}}\|_H^2$, i.e. the squared distance between \hat{y} and y_{True} , weighted by the distance matrix H . Because there is no clear way to simulate a “true” regression coefficient β_{True} in this example, we do not compare the estimation performance of KPR and ridge. Tuning parameters in this example are also chosen using 10-fold cross-validation. For KPR, we find the tuning parameters that minimize the sum of squared test error weighted by H ; for ridge, we completely ignore the information in H and find the tuning parameters that minimize the squared test error. Figure 3 shows that KPR outperformed ridge regression in prediction in all settings.

3.3 Regression and PCoA using an edge-matrix kernel

In this section, our simulations are based on data from a study of bacterial vaginosis (BV) by Srinivasan et al. [58] in which 16S rRNA gene samples were collected from vaginal swabs in $n = 220$ women with and without BV. Here, the outcome y represents pH measured from vaginal fluid of each subject and we consider the association of y with genus-level taxa. In this example, we use the $p = 62$ genera that exhibit non-zero sequence counts in at least 20%

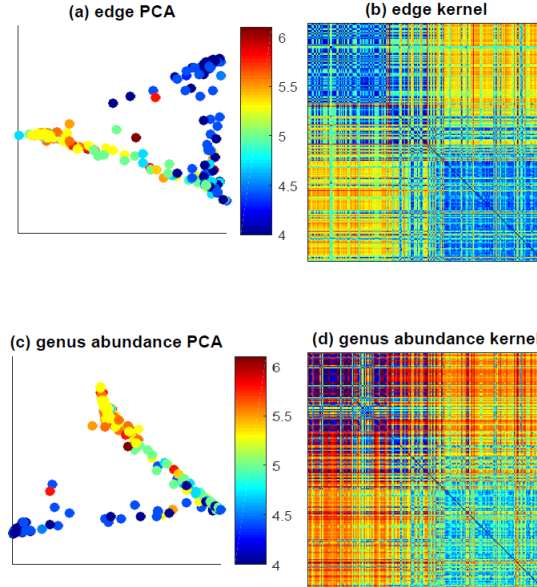


Figure 4: **Analysis of bacterial vaginosis data from [58].** (a): representation of the samples in the space of the first two PC’s of the edge-matrix kernel $H = EE'$. The color of each point corresponds to the pH level of the sample; (b): heatmap of edge-matrix kernel used to generate the plot in (a); (c): two-dimensional PCA plot based on the genus-level relative abundances; (d): heatmap of the genus-abundance kernel $K = XX'$ used to create the plot in (c). In (b) and (d), subjects are ordered by the pH values.

of the subjects and so X denotes a 220×62 sample-by-genus matrix. For the KPR model, we define a kernel H based on the “edge mass difference matrix”, E , introduced by Matsen and Evans [46]. Specifically, if the full phylogenetic tree has q edges, each sample can be represented by a vector indexed by all q edges, the e^{th} coordinate of which quantifies the difference between the fraction of sequence reads on either side of the edge; i.e., the fraction of reads observed on the root side of the tree minus the fraction of reads on the non-root side. We refer to [46] for details and a discussion of “edge PCA”, which refers to PCA applied to the $n \times q$ matrix E . Note, in particular, that abundances from *every* taxon level in the tree contribute to a similarity between subjects as opposed to abundances at a single taxon level, as with UniFrac or DPCoA. Here, E is based on all $q = 1770$ edges in the original phylogenetic tree, and Figure 4(a) shows a PCA plot of the 220 subjects in which their similarity is defined using the kernel $H = EE'$; the color of each dot represents the subject’s pH.

Figure 4(b) is a heatmap of the kernel H used to create Figure 4(a). The columns and rows of H represent similarities between samples based on the edge mass difference matrix, ordered by subject pH measurement. Similarly, Figure 4(c) is a PCA plot based on similarities defined using the genus-level abundance kernel, $K = XX'$. Figure 4(d) is a heatmap of the kernel K used to create Figure 4(c), and subjects are again ordered by pH. These figures illustrate how two different measures of similarity (two separate kernels) may be co-informative in the sense that they both provide information about grouping of subjects’ microbiota in relation to their pH. It is thus natural to expect that incorporating information from both H and K within the KPR framework may result in improved estimates of association between $y = \text{pH}$ and the taxon abundances.

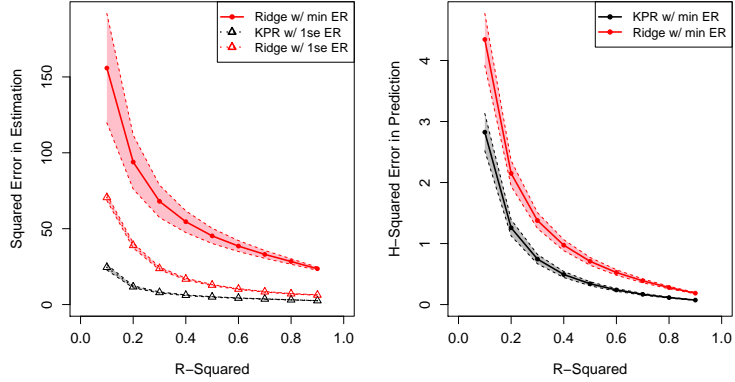


Figure 5: average estimation squared error and prediction H -squared error of KPR (black) and ridge regression (red), and their 95% confidence bands. Tuning parameters are those that produce the smallest test error (min ER), and the largest ones such that the test errors are within one standard error of the minimum test error (1se ER).

For the simulation, we define a “true” association between pH and the genus-level taxa by using the 2-dimensional PCR model eq. (3). Specifically, we use the apparent association between $y = \text{pH}$ and genus-level abundances in Figure 4(c) to construct a plausible “true” coefficient vector β_{True} for simulation. That is, β_{True} is defined as the PCR estimate from the first two principal components of X as in eq. (3) (cf., Figure 1(b)).

Taking $H = EE'$ in a KPR model of the form (12), we compare the resulting estimate of β with a ridge estimate. The performance metrics are estimation squared error and prediction H -squared error, defined in Section 3.2 as $\|\hat{y} - y_{\text{True}}\|_H^2$. Tuning parameters are selected using 10-fold cross-validation. For KPR, we find the tuning parameters that minimize the sum of squared test error weighted by H ; for ridge, we completely ignore the information of H and find the tuning parameters that minimize the sum of squared test error. As in section 3.1, we also allowed for using the largest tuning parameters such that the squared test error is within one standard error of the minimum squared test error. We repeated the simulation 400 times. Figure 5 shows that KPR significantly outperforms ridge regression in both prediction and estimation. Again, ridge regression with the larger tuning parameter (within one on standard error of the minimum) performs better in estimation than simply using the smallest squared test error.

4 Analysis of an observational study

We apply our kernel-penalized regression framework to 16S rRNA gene data from a study of premenopausal women [30]. This study evaluated the association between urinary enterolignan excretion and the gut microbial communities in stool samples from 115 premenopausal (ages 40 to 45 years) women in the United States. The gut microbiota was evaluated using 454 pyrosequencing of the 16S rRNA gene. Sequences were aligned in SILVA (www.arb-silva.de). Operational taxonomic units (species) were identified at 97% sequence similarity. We evaluated the association of percent body fat (as measured using dual energy X-ray absorptiometry;

Table 1: Species found (in increasing order of p-values) to be associated with percent fat at different significant levels by KPR with CLR transformed abundances, ridge and lasso regression with CLR transformed abundances, and ridge and lasso regressions with untransformed relative abundances (rel%).

	$p < 0.01$	$p < 0.005$	$FDR < 0.1$
KPR with CLR	Bacteroides, Turicibacter, Acidaminococcus, Dethiosulfatibacter, Asaccharobacter, Anaerovorax, Blautia, Lebetimonas, Streptobacillus, Anoxynatronum	Bacteroides, Turicibacter, Acidaminococcus, Dethiosulfatibacter	(none)
Ridge with CLR	(none)	(none)	(none)
Ridge with rel%	Catonella, Dethiosulfatibacter	(none)	(none)
Lasso with CLR	Roseburia	(none)	(none)
Lasso with rel%	Dethiosulfatibacter, Micropruina	Dethiosulfatibacter	(none)

Hologic Delphi, Hologic Inc.) with species. Thirteen subjects had missing outcome (percent body fat) values and were removed from analysis. The relative abundances of 127 species were zero for more than 90% of the subjects. Those 127 species may not provide much information in analysis, and were also removed from analysis. The resulting data set consists of $n = 102$ observations for $p = 128$ species.

To make the measurements comparable between subjects, the species abundances were scaled by the total number of sequences measured in each sample. This scaling produces compositional data (the relative abundances in each sample sum to 1) which, as discussed in section 2.4, imposes analytical complications. In particular, regression analysis using compositional covariates must somehow account for their unit sum constraint [36, 39]. For this reason, we applied the CLR transformation to the relative abundance values and this transformed data \tilde{X} is used as the matrix of predictors in the KPR model. Additionally, using Aitchison's variation matrix [3], T , we obtained the covariance matrix, C , as described in section 2.4. As C provides more accurate information on the covariance of the log-transformed true abundances than does the empirical covariance matrix from relative abundances, X , or their CLR transform, \tilde{X} , we use C in place of Q in (6).

In this example, we examined the effect of using the CLR transformed data and covariance C as in (15) and fit penalized regression models with the goal of identifying specific species that may be associated with adiposity, as measured by percent body fat in the cohort of subjects described above. To this end, we applied an inference procedure to three high-dimensional models in order to identify species exhibiting evidence of association with subjects' adiposity. This significance test for graph-constrained estimation, called Grace [70], provides a means to assign significance to penalized regression models that incorporate structure of the type provided by Q in (6) (or C in (15)). The method asymptotically controls the type-I error rate regardless of the choice of Q . The special case with $Q = I$ provides a significance test for ordinary ridge regression. In each application of the Grace test, tuning parameters were selected based on the smallest squared test error using 10-fold cross validation. Following [70], the sparsity parameter is set to be $\xi = 0.05$, and the tuning parameter for the initial estimator set to $\lambda_{init} = 4\hat{\sigma}_\epsilon\sqrt{3\log p/n}$. The standard deviation of the random error ϵ , denoted

$\hat{\sigma}_\epsilon$, was estimated using the scaled Lasso [59]. As an alternative to ridge, and to account for the possibility of sparse models, we also considered the recently proposed significance tests for lasso regressions based on low-dimensional projection estimator (LDPE) [68, 65], which provides an asymptotically valid test for lasso-penalized regression estimates.

We examined five estimation methods: (i) ordinary ridge and (ii) lasso regressions using the relative abundance vectors in the matrix of predictors, X ; (iii) ridge and (iv) lasso regressions using the CLR transformed vectors in the matrix of predictors, \tilde{X} ; and (v) the KPR model in (15). None of these models resulted in any species associated with percent fat when controlled for false discovery rate (FDR) at 0.1 using the Benjamini-Yekutieli procedure [5]. However, when using a cut-off of $p = 0.01$, the KPR model resulted in ten species associated with adiposity. This model also resulted in four species with a cut-off of $p = 0.005$. Ordinary ridge regressions using the CLR-transformed vectors found no associations at a cut-off of $p = 0.01$, whereas using the relative abundances, ridge found two species at the $p = 0.01$ cut-off and none at $p = 0.005$. Lasso regression with the CLR-transformed vectors identified one species at the $p = 0.01$ cut-off and none at $p = 0.005$ cut-off. When using the relative abundances, lasso identified two species as significant at the $p = 0.01$ cut-off and one at the $p = 0.005$ cutoff. See Table 1 for the list of identified species.

5 Discussion

We have formulated a family of regression models that naturally build on the dimension-reduced graphical explorations common to microbiome studies. In this sense, we have simply re-considered multivariate ordination methods and carried them to their logical conclusion by emphasizing the role of the eigenanalysis in these penalized regression models. Said another way, the large family of models developed here are a statistical, supervised-learning counterpart to the unsupervised methods of principal coordinate analysis.

One of the primary motivations for PCoA graphical displays is the ability to incorporate biologically-inclined measures of (dis)similarity. The popular use of UniFrac, for instance, is motivated by the desire to impose phylogeny into the analysis. These dissimilarities have also been used for rigorous statistical testing in the context of MANOVA [4] or the closely-related kernel machine regression score test [26, 50, 7, 69] for global association of a multivariate predictor with an outcome. However, the use of UniFrac and other non-Euclidean distances make it difficult to identify specific associations between the microbial abundance profiles and a phenotype and, indeed, none of these analyses proceed to estimate these individual associations. In addition to ordination displays and global tests for associations, a variety of machine learning approaches are focused on models that *predict* a response. In contrast, here we have emphasized coefficient-vector *estimation*, an important aspect of any interpretable model for the association of microbial communities with an outcome or phenotype. An interesting aspect of this framework is the ability to sidestep some of the problems inherent in compositional data analysis. Indeed, as emphasized by Li [39] regression analysis with compositional covariates must somehow acknowledge their unit-sum constraint and spurious correlations. Our approach, which differs somewhat from that of Li [39], might be viewed as a penalized version of the linear model for compositions by Tolosana-Delgado and van den Boogaart [64] where our high-dimensional model additionally incorporates statistical significance for estimated regression coefficients.

References

- [1] J. Aitchison, *A concise guide to compositional data analysis*, 2nd Compositional Data Analysis Workshop; Girona, Italy, 2003.
- [2] _____, *The statistical analysis of compositional data*, Blackburn Press, New Jersey, 2003.
- [3] John Aitchison, *The statistical analysis of compositional data*, Journal of the Royal Statistical Society. Series B (Methodological) (1982), 139–177.
- [4] M.J. Anderson, *Distance-based tests for homogeneity of multivariate dispersions*, *Biometrics* **62** (2006), no. 1, 245–253.
- [5] Y. Benjamini and D. Yekutieli, *The control of the false discovery rate n multiple testing under dependency*, *The Annals of Statistics* **29** (2001), no. 4, 1165–1188.
- [6] T. T. Cai and P. Hall, *Prediction in functional linear regression*, *The Annals of Statistics* **34** (2006), no. 5, 2159–2179.
- [7] J. Chen, K. Bittinger, E.S. Charlson, C. Hoffmann, J. Lewis, G.D. Wu, R.G. Collman, F.D. Bushman, and H. Li, *Associating microbiome composition with environmental covariates using generalized UniFrac distances*, *Bioinformatics* **28** (2012), no. 16, 2106–2113.
- [8] M. Chen, J. Cho, and H. Zhao, *Incorporating biological pathways via a markov random field model in genome-wide association studies*, *PLoS Genetics* **7** (2011), no. 4, e1001353.
- [9] I. Cho, S. Yamanishi, L. Cox, B.A. Methé, J. Zavadil, K. Li, Z. Gao, D. Mahana, K. Raju, I. Teitler, et al., *Antibiotics in early life alter the murine colonic microbiome and adiposity*, *Nature* **488** (2012), no. 7413, 621–626.
- [10] M.J. Claesson, I.B. Jeffery, S. Conde, S.E. Power, E.M. O'Connor, S. Cusack, H.M.B. Harris, M. Coakley, B. Lakshminarayanan, O. OSullivan, et al., *Gut microbiota composition correlates with diet and health in the elderly*, *Nature* **488** (2012), no. 7410, 178–184.
- [11] Human Microbiome Project Consortium et al., *Structure, function and diversity of the healthy human microbiome*, *Nature* **486** (2012), no. 7402, 207–214.
- [12] P.B. Eckburg, E.M. Bik, C.N. Bernstein, E. Purdom, L. Dethlefsen, M. Sargent, S.R. Gill, K.E. Nelson, and D.A. Relman, *Diversity of the human intestinal microbial flora*, *Science* **308** (2005), no. 5728, 1635–1638.
- [13] D.M. Endres and J.E. Schindelin, *A new metric for probability distributions*, *Information Theory, IEEE Transactions on* **49** (2003), no. 7, 1858–1860.
- [14] Y. Escoufier, *Operator related to a data matrix: a survey*, *Compstat 2006-Proceedings in Computational Statistics* (2006), 285–297.
- [15] S.N. Evans and F.A. Matsen, *The phylogenetic Kantorovich–Rubinsteiin metric for environmental sequence samples*, *Journal of the Royal Statistical Society: Series B* **74** (2012), no. 3, 569–592.

- [16] K. Faust, J.F. Sathirapongsasuti, J. Izard, N. Segata, D. Gevers, J. Raes, and C. Huttenhower, *Microbial co-occurrence relationships in the human microbiome*, PLoS Comput Biol **8** (2012), no. 7, e1002606–e1002606.
- [17] J.N. Franklin, *Minimum principles for ill-posed problems*, SIAM Journal on Mathematical Analysis **9** (1978), no. 4, 638–650.
- [18] J. Friedman and E.J. Alm, *Inferring correlation networks from genomic survey data*, PLoS Computational Biology **8** (2012), no. 9, e1002687.
- [19] J. Fukuyama, P.J. McMurdie, L. Dethlefsen, D.A. Relman, and S. Holmes, *Comparisons of distance methods for combining covariates and abundances in microbiome studies*, Pac Symp Biocomput, 2012.
- [20] G.H. Golub and C.F. Van Loan, *Matrix computations*, Johns Hopkins University Press, Baltimore, MD, 2012.
- [21] J.K. Goodrich, S.C. Di Rienzi, A.C. Poole, O. Koren, W.A. Walters, J.G. Caporaso, R. Knight, and R.E. Ley, *Conducting a microbiome study*, Cell **158** (2014), no. 2, 250–262.
- [22] M.J. Greenacre, *Theory and applications of correspondence analysis*, Academic Press, 1984.
- [23] A. Gretton, K. Fukumizu, C.H. Teo, L. Song, B. Schölkopf, and A.J. Smola, *A kernel statistical test of independence*, Advances in Neural Information Processing Systems: Proceedings of the 2007 Conference (Cambridge, MA), MIT Press, 2008, pp. 585–592.
- [24] A. Gretton, R. Herbrich, A. Smola, O. Bousquet, and B. Schölkopf, *Kernel methods for measuring independence*, The Journal of Machine Learning Research **6** (2005), 2075–2129.
- [25] M. Hamady and R. Knight, *Microbial community profiling for human microbiome projects: Tools, techniques, and challenges*, Genome research **19** (2009), no. 7, 1141–1152.
- [26] F. Han and W. Pan, *Powerful multi-marker association tests: unifying genomic distance-based regression and logistic regression*, Genetic epidemiology **34** (2010), no. 7, 680–688.
- [27] P.C. Hansen, *Rank-Deficient and Discrete Ill-Posed Problems*, SIAM, Philadelphia, PA, 1998.
- [28] T. Hastie, R. Tibshirani, and J. Friedman, *The elements of statistical learning: Data mining, inference, and prediction*, Springer-Verlag, New York, 2009.
- [29] A.E. Hoerl and R.W. Kennard, *Ridge regression: Biased estimation for nonorthogonal problems*, Technometrics **12** (1970), no. 1, 55–67.
- [30] M.A.J. Hullar, S.M. Lancaster, F. Li, E. Tseng, K. Beer, C. Atkinson, K. Wähälä, W.K. Copeland, T.W. Randolph, K.M. Newton, et al., *Enterolignan-producing phenotypes are associated with increased gut microbial diversity and altered composition in pre-menopausal women in the united states*, Cancer Epidemiology Biomarkers & Prevention **24** (2015), no. 3, 546–554.

- [31] J. Josse and S. Holmes, *Measures of dependence between random vectors and tests of independence*, (2013), <http://arxiv.org/abs/1307.7383v2>.
- [32] J. Josse, J. Pagès, and F. Husson, *Testing the significance of the RV coefficient*, Computational Statistics & Data Analysis **53** (2008), no. 1, 82–91.
- [33] S. Kim and E.P. Xing, *Tree-guided group lasso for multi-task regression with structured sparsity*, Proceedings of the 27th International Conference on Machine Learning (Haifa, Israel), 2010.
- [34] O. Koren, D. Knights, A. Gonzalez, L. Waldron, N. Segata, R. Knight, C. Huttenhower, and R.E. Ley, *A guide to enterotypes across the human body: meta-analysis of microbial community structures in human microbiome datasets*, PLoS Computational Biology **9** (2013), no. 1, e1002863.
- [35] J. Kuczynski, Z. Liu, C. Lozupone, D. McDonald, N. Fierer, and R. Knight, *Microbial community resemblance methods differ in their ability to detect biologically relevant patterns*, Nature methods **7** (2010), no. 10, 813–819.
- [36] Z.D. Kurtz, C.L. Mueller, E.R. Miraldi, D.R. Littman, M.J. Blaser, and R.A. Bonneau, *Sparse and compositionally robust inference of microbial ecological networks*, PLoS Computational Biology **11** (2015), no. 5, e1004226.
- [37] R.E. Ley, C.A. Lozupone, M. Hamady, R. Knight, and J.I. Gordon, *Worlds within worlds: evolution of the vertebrate gut microbiota*, Nature Reviews Microbiology **6** (2008), no. 10, 776–788.
- [38] C. Li and H. Li, *Network-constrained regularization and variable selection for analysis of genomic data*, Bioinformatics **24** (2008), no. 9, 1175.
- [39] H. Li, *Microbiome, metagenomics, and high-dimensional compositional data analysis*, Annual Review of Statistics and Its Application **2** (2015), no. 1, 73–94.
- [40] C.F. Van Loan, *Generalizing the singular value decomposition*, SIAM J. Numerical Analysis **13** (1976), no. 1, 76–83.
- [41] D. Lovell, V. Pawlowsky-Glahn, J.J. Egozcue, S. Marguerat, and J. Bähler, *Proportionality: a valid alternative to correlation for relative data*, PLoS computational biology **11** (2015), no. 3, e1004075.
- [42] C. Lozupone and R. Knight, *UniFrac: a new phylogenetic method for comparing microbial communities*, Applied and environmental microbiology **71** (2005), no. 12, 8228–8235.
- [43] C.A. Lozupone, M. Hamady, S.T. Kelley, and R. Knight, *Quantitative and qualitative β diversity measures lead to different insights into factors that structure microbial communities*, Applied and environmental microbiology **73** (2007), no. 5, 1576–1585.
- [44] C.A. Lozupone and R. Knight, *Species divergence and the measurement of microbial diversity*, FEMS Microbiology Reviews **32** (2008), no. 4, 557–578.

[45] David G Luenberger, *Optimization by vector space methods*, John Wiley & Sons, New York, NY, 1969.

[46] F.A Matsen and S.N. Evans, *Edge principal components and squash clustering: using the special structure of phylogenetic placement data for sample comparison*, PLoS ONE **8** (2013), no. 3, e56859.

[47] P.J. McMurdie and S. Holmes, *phyloseq: an R package for reproducible interactive analysis and graphics of microbiome census data*, PloS one **8** (2013), no. 4, e61217.

[48] B.D Muegge, J. Kuczynski, D. Knights, J.C. Clemente, A. González, L. Fontana, B. Henrissat, R. Knight, and J.I. Gordon, *Diet drives convergence in gut microbiome functions across mammalian phylogeny and within humans*, Science **332** (2011), no. 6032, 970–974.

[49] C.C. Paige and M.A. Saunders, *Towards a generalized singular value decomposition*, SIAM J. Numerical Analysis **18** (1981), no. 3, 398–405.

[50] W. Pan, *Relationship between genomic distance-based regression and kernel machine regression for multi-marker association testing*, Genetic Epidemiology **35** (2011), no. 4, 211–216.

[51] S. Pavoine, A-B. Dufour, and D. Chessel, *From dissimilarities among species to dissimilarities among communities: a double principal coordinate analysis*, Journal of Theoretical Biology **228** (2004), no. 4, 523–537.

[52] Vera Pawlowsky-Glahn and Antonella Buccianti, *Compositional data analysis: Theory and applications*, John Wiley & Sons, 2011.

[53] E. Pekalska, P. Paclik, and R.P.W. Duin, *A generalized kernel approach to dissimilarity-based classification*, The Journal of Machine Learning Research **2** (2002), 175–211.

[54] E. Purdom, *Analysis of a data matrix and a graph: Metagenomic data and the phylogenetic tree*, The Annals of Applied Statistics **5** (2011), no. 4, 2326–2358.

[55] A. Ramette, *Multivariate analyses in microbial ecology*, FEMS Microbiology Ecology **62** (2007), no. 2, 142–160.

[56] T.W. Randolph, J. Harezlak, and Z. Feng, *Structured penalties for functional linear models: partially empirical eigenvectors for regression*, Electronic journal of statistics **6** (2012), 323.

[57] B. Schölkopf and A.J. Smola, *Learning with kernels: Support vector machines, regularization, optimization, and beyond*, MIT Press, Cambridge, MA, 2002.

[58] S. Srinivasan, N.G. Hoffman, M.T. Morgan, F.A. Matsen, T.L. Fiedler, R.W. Hall, F.J. Ross, C.O. McCoy, R. Bumgarner, J.M. Marrazzo, et al., *Bacterial communities in women with bacterial vaginosis: high resolution phylogenetic analyses reveal relationships of microbiota to clinical criteria*, PloS one **7** (2012), no. 6, e37818.

[59] T. Sun and C.-H. Zhang, *Scaled sparse linear regression*, Biometrika **99** (2012), no. 4, 879–898.

[60] G.J. Székely, M.L. Rizzo, and N.K. Bakirov, *Measuring and testing dependence by correlation of distances*, The Annals of Statistics **35** (2007), no. 6, 2769–2794.

[61] O. Tanaseichuk, J. Borneman, and T. Jiang, *Phylogeny-based classification of microbial communities*, Bioinformatics **30** (2014), no. 4, 449–456.

[62] R. Tibshirani, *Regression shrinkage and selection via the lasso*, Journal of the Royal Statistical Society B **58** (1996), no. 1, 267–288.

[63] R.J. Tibshirani and J Taylor, *The solution path of the generalized lasso*, The Annals of Statistics **39** (2011), no. 3, 1335–1371”.

[64] Raimon Tolosana-Delgado, KG Van Den Boogart, V Pawlowsky-Glahn, and A Buccianti, *Linear models with compositions in R*, Compositional data analysis: Theory and applications, John Wiley and Sons, New York, 2011, pp. 356–371.

[65] S. Van de Geer, P. Bühlmann, Y. Ritov, R. Dezeure, et al., *On asymptotically optimal confidence regions and tests for high-dimensional models*, The Annals of Statistics **42** (2014), no. 3, 1166–1202.

[66] J. Wessel and N.J. Schork, *Generalized genomic distance-based regression methodology for multilocus association analysis*, The American Journal of Human Genetics **79** (2006), no. 5, 792–806.

[67] T. Yatsunenko, F.E. Rey, M.J. Manary, I. Trehan, M.G. Dominguez-Bello, M. Contreras, M. Magris, G. Hidalgo, R.N. Baldassano, A.P. Anokhin, et al., *Human gut microbiome viewed across age and geography*, Nature **486** (2012), no. 7402, 222–227.

[68] C.-H. Zhang and Stephanie S. Zhang, *Confidence intervals for low dimensional parameters in high dimensional linear models*, Journal of the Royal Statistical Society: Series B (Statistical Methodology) **76** (2014), no. 1, 217–242.

[69] N. Zhao, J. Chen, I.M. Carroll, T. Ringel-Kulka, M.P. Epstein, H. Zhou, J.J. Zhou, Y. Ringel, H. Li, and M.C. Wu, *Testing in microbiome-profiling studies with MiRKAT, the microbiome regression-based kernel association test*, The American Journal of Human Genetics **96** (2015), no. 5, 797–807.

[70] S. Zhao and A. Shojaie, *A significance test for graph-constrained estimation*, Biometrics **to appear** (2015).

[71] H. Zou and T. Hastie, *Regularization and variable selection via the elastic net*, JRSSB **67** (2005), no. 2, 301–320.